The Retinal Ganglion Cell Response to Blast-Mediated Traumatic Brain Injury Is Genetic Background Dependent

Matthew M. Harper,[1,2] Nickolas Boehme,[1,2] Laura M. Dutca,[1,2] and Michael G. Anderson[1–3]

[1]Department of Ophthalmology and Visual Sciences, Carver College of Medicine, The University of Iowa, Iowa City, IA, United States
[2]Center for the Prevention and Treatment of Visual Loss, Iowa City VA Healthcare System, Department of Veterans Affairs, Iowa City, IA, United States
[3]The Department of Molecular Physiology and Biophysics, Carver College of Medicine, The University of Iowa, Iowa City, IA, United States

Correspondence: Matthew M. Harper, VA Center for the Prevention and Treatment of Visual Loss, Department of Ophthalmology and Visual Sciences, The University of Iowa, 601 Hwy 6 W, Iowa City, 52242, IA, USA; matthew-harper@uiowa.edu.

Received: November 26, 2020
Accepted: May 9, 2021
Published: June 9, 2021

Citation: Harper MM, Boehme N, Dutca LM, Anderson MG. The retinal ganglion cell response to blast-mediated traumatic brain injury is genetic background dependent. *Invest Ophthalmol Vis Sci.* 2021;62(7):13. https://doi.org/10.1167/iovs.62.7.13

Purpose. The purpose of this study was to examine the influence of genetic background on the retinal ganglion cell (RGC) response to blast-mediated traumatic brain injury (TBI) in Jackson Diversity Outbred (J:DO), C57BL/6J and BALB/cByJ mice.

Methods. Mice were subject to one blast injury of 137 kPa. RGC structure was analyzed by optical coherence tomography (OCT), function by the pattern electroretinogram (PERG), and histologically using BRN3A antibody staining.

Results. Comparison of the change in each group from baseline for OCT and PERG was performed. There was a significant difference in the J:DOΔOCT compared to C57BL/6J mice ($P = 0.004$), but not compared to BALB/cByJ ($P = 0.21$). There was a significant difference in the variance of the ΔOCT in J:DO compared to both C57BL/6J and BALB/cByJ mice. The baseline PERG amplitude was 20.33 $\pm$ 9.32 µV, which decreased an average of -4.14 ± 12.46 µV following TBI. Baseline RGC complex + RNFL thickness was 70.92 $\pm$ 4.52 µm, which decreased an average of -1.43 ± 2.88 µm following blast exposure. There was not a significant difference in the ΔPERG between J:DO and C57BL/6J ($P = 0.13$), although the variances of the groups were significantly different. Blast exposure in J:DO mice results in a density change of 558.6 $\pm$ 440.5 BRN3A-positive RGCs/mm^2 (mean $\pm$ SD).

Conclusions. The changes in retinal outcomes had greater variance in outbred mice than what has been reported, and largely replicated herein, for inbred mice. These results demonstrate that the RGC response to blast injury is highly dependent upon genetic background.

Keywords: blast, vision, retinal ganglion cells, traumatic brain injury, neurotrauma, pattern electroretinogram, genetic variation

Traumatic brain injury (TBI) is a significant public health concern that accounts for over 2.8 million emergency room visits per year in the United States.[1] The leading causes for TBI include falls, motor vehicle accidents, and being struck by or against an object.[1,2] One common cause of TBI in military personnel is exposure to blast. A history of exposure to blast injuries is common among veterans. Nearly 75% of combat-related injuries in recent military conflicts were due to explosive devices[3] and nearly 50% of such blast injuries resulted in mild TBI.[4]

Damage from primary blast injuries results from an overpressure wave passing through tissues, with the central nervous system being particularly prone to damage. Many individuals who suffer from TBI also report symptoms of visual dysfunction with retinal pathology, which can present either acutely or chronically after the initial injury.[5,6] One recent analysis of diagnostic codes for visual field loss of veterans with documented TBI calculated that the incidence of visual dysfunction was approximately 8.6%.[7] Although TBI patients report a wide range of visual disturbances, little is known about the molecular changes that initiate neuronal dysfunction that cause defects in vision.

Regardless of the cause of TBI, many studies have shown significant differences in outcomes between patients with similar injuries. The variability in patient outcomes may be due to the differences in medical care and therapy available to each patient.[8,9] However, growing evidence has suggested that an individual's response to and recovery from TBI is closely linked to genetic predisposition.[10–12] Indeed, multiple genes have been identified that may influence function after TBI, including those related to apolipoprotein E, brain-derived neurotrophic factor, the dopaminergic system, the serotonergic system, and interleukins, among others.[13] These genes have been shown to influence many psychiatric parameters, including cognition, working memory, executive dysfunction, aggression, inhibition, and impulsiveness[9]—and suggest that there is not a singular molecular or anatomical response to TBI.

While studies of humans with blast injury have shown differences among individuals, it is unknown whether this is due to time after injury, differences in the type of injury, or differences in genetic composition. Studies in preclinical models of blast injury have shown differences in visual responses between inbred strains,[14] and have utilized differences in BXD inbred strains to monitor transcriptional changes after blast exposure.[15] However, analysis of visual function has not yet been performed following blast injury in outbred strains of mice to evaluate the interaction of genetic composition and blast exposure. An outbred stock of mice that was recently developed is the Jackson Diversity Outbred (J:DO) mouse. J:DO mice have a high degree of genetic heterogeneity. The J:DO stock was generated by crosses between 144 early generation recombinant inbred lines contributing to the Collaborative Cross,[16] and thus incorporates similar genetic variation, including variation from all the major phylogenetic branches present in laboratory mice. The founder lines include wild-derived CAST/EiJ, PWK/PhJ, and WSB/EiJ; and inbred C57BL/6J, 129S1/SvlmJ, NOD/ShiLtJ, NZO/HiLtJ, and A/J. J:DO mice lack known overt retinal degenerative mutations, such as *rd1* or *rd8,*[17,18] and have normal appearing retinas.[19] J:DO have approximately 45 million segregating genetic variations and encompass the majority of all existing genetic diversity in laboratory strains of mice. J:DO mice have had multiple generations of opportunity for meiotic recombination, which makes them useful for analysis of complex traits,[20–24] such as the response to blast.

The principal purpose of this study was to determine if genetic composition influences the phenotypic RGC response to blast-mediated TBI. Here we use the J:DO mouse strain that has more genetic complexity than inbred mice to evaluate the influence of genetic background on visual responses to blast exposure.

Methods

Animals

All animal studies were conducted in accordance with the ARVO Statement for the Use of Animals in Ophthalmic and Vision Research and were approved by the Iowa City Department of Veterans Affairs Institutional Animal Care and Use Committee. Male J:DO, C57BL/6J and BALB/cByJ mice were purchased from The Jackson Laboratory and subjected to blast injury at eight weeks of age. Data from C57BL/6J mice used in this manuscript were reanalyzed and displayed in a different manner from our previous studies.[25] A total of 81 mice (male, eight weeks old at the time of blast exposure) were used for the purpose of this study: $n = 57$ J:DO, $n = 12$ C57BL/6J, and $n = 12$ BALB/cByJ.

Blast Injury Induction

An enclosed blast chamber was used for these studies, one half of which was pressurized, with a 13 cm diameter opening between the chamber halves, as described previously.[25–33] A Mylar membrane (Mylar A, 0.00142 gauge; Country Plastics, Ames, IA) was placed over the opening on the pressurized side of the chamber. The unpressurized side of the tank contained a padded polyvinyl chloride (PVC) protective restraint for positioning of an anesthetized mouse (see Mohan et al., 2013[26] for diagram). To create the blast wave, air was pumped into the pressurized side of the tank to 20 PSI. Using this model, a blast wave is produced with the following characteristics after rupture of 20 PSI membranes: 140.92 ± 10.82 kPa peak pressure with a 7.0 ± 2.09 ms positive phase duration. The pressure was measured using a sensor of 1 cm in diameter placed directly below the head of the mouse. Prior to blast wave induction, mice were anesthetized with a combination of ketamine (30 mg/kg body weight, intraperitoneal, IP) and xylazine (5 mg/kg body weight, IP) and positioned within the unpressurized half of the blast chamber with the left side of the head oriented toward the source of the blast wave. Only the head of the mouse was exposed to the blast wave, with the rest of the body shielded. The head of the mouse was unrestrained during blast wave exposure but was prevented in coming into contact with any hard surface by thick foam placed directly behind the head. After blast exposure, mice were placed on a heating pad to facilitate recovery from general anesthesia and to prevent hypothermia. Xylazine anesthesia was reversed with yohimbine chloride (1 mg/kg, IP). Mice received analgesic via subcutaneous injection (0.1 mL/20 g body weight) of buprenorphine (0.003 mg/mL) immediately after recovery from the procedure. Mice were analyzed four weeks following blast exposure, and tissue was collected.

Pattern Evoked Electroretinography

Pattern evoked electroretinography (PERG) was used to objectively measure the function of RGCs by recording the amplitude of the PERG waveform at baseline, and again four weeks following blast exposure. Mice were anesthetized with a combination of ketamine (30 mg/kg, IP), xylazine (5 mg/kg, IP), and acepromazine (2 mg/kg, IP) and were placed on a heated animal holder. Binocular PERG responses were evoked using alternating, reversing, black and white vertical stimuli delivered on an LED monitor (Jorvec, Miami, FL), as described by Chou et al.[34] A subdermal recording electrode was placed under the skin on the nose of the animal extending to the snout, equidistant from each eye, as previously described.[25,29–31,34–36] A reference needle electrode was placed at the base of the head, and a ground electrode was placed at the base of the tail to complete the circuit. Each animal was placed at the same fixed position, with the eyes positioned 10 cm from the stimulus monitor to prevent recording variability due to animal placement. Stimuli (18° radius visual angle subtended on full field pattern, 1.5 cm high × 14 cm wide bars, two reversals per second, 372 averaged signals with cutoff filter frequencies of 1 to 30 Hz, 98% contrast, 80 cd/m^2 average monitor illumination intensity using luminance matched pattern reversals to exclude outer retinal contributions) were delivered under mesopic conditions (8.5 lux room luminance) without dark adaptation. A diffuser placed over the pattern on the monitor did not elicit a measurable evoked potential, further ensuring that the electrical responses were elicited from retinal ganglion cells. The PERG response was evaluated by measuring the amplitude (peak to trough) and implicit time of the waveform, as previously described.[35,37] Data preblast are presented from both eyes. Data postblast are presented from the left eye, which was directly exposed to blast injury. The PERG was recorded in an identical manner pre- and postblast. Mice were examined with a hand-held slit lamp prior to PERG analysis to ensure that no anterior segment damage was present. The change in PERG response (ΔPERG) is the difference in the PERG amplitude at four weeks postblast injury compared to baseline responses in the same animal.

Only PERG recordings that resulted in a waveform consistent with the PERG response were used for the purpose of this study.

Spectral Domain Optical Coherence Tomography

Spectral domain optical coherence tomography (SD-OCT) analysis was performed using a Spectralis SD-OCT (Heidelberg Engineering, Vista, CA) imaging system coupled with a 25D lens for mouse ocular imaging[35] (Heidelberg Engineering, Vista, CA). Mice were anesthetized with a combination of ketamine (30 mg/kg, IP) and xylazine (5 mg/kg, IP) and placed on a heating pad to maintain body temperature. Pupils were dilated using a 1% tropicamide solution. The cornea was moisturized with a saline solution. Volume scans (49-line dense array, 15 A-scans per B-scan, 20° scan angle, 20° × 25° scan area) positioned directly over the optic nerve head were performed to quantify the retinal ganglion cell complex + RNFL thickness (RNFL + GCL + IPL). One single B-scan was analyzed by an individual masked to the treatment of the mouse in the superior retina, approximately 150 µm from the peripapillary region. All scans were analyzed by excluding blood vessels from the RGC complex + RNFL thickness calculation. The RGC complex + RNFL thickness was analyzed at baseline, and then again four weeks following blast exposure. The change in OCT thickness (ΔOCT) was evaluated by determining the difference in the RGC complex + RNFL thickness four weeks post blast injury compared to baseline responses in the same animal. Only OCT scans that had a clarity of at least 26, as measured by Heidelberg Spectralis were used for the purpose of this study.

Immunohistochemical-Based RGC Quantification

To calculate the change in RGC density in J:DO mice, the right eye of each animal was enucleated prior to blast injury (Supplementary Fig. S1) and processed as described below. For surgical unilateral enucleation, mice were anesthetized with a combination of ketamine (100 mg/kg, IP) and xylazine (10 mg/kg, IP). The surgical area was cleaned with alcohol and chlorhexidine, and the right eye was enucleated. Following enucleation, the right eye socket was cauterized, and the lid sutured shut. Antibiotic ointment was applied to the area. Immediately following enucleation, mice was placed on a warming pad to maintain body temperature and given buprenorphine for three days following enucleation (0.1 mg/kg, subcutaneous) to prevent any pain.

Enucleation was necessary to calculate the RGC change in density, as each J:DO mouse has a unique genetic constitution[23,38] and RGC number is genetic background dependent.[39] Thus, it was expected that the two eyes of an individual mouse would have a similar number of RGCs (because they share the same genetic background) but differ between animals (because outbred mice have differing genetic backgrounds), making it necessary to consider RGC parameters on a per mouse basis. Four weeks following blast exposure, mice were euthanized, whole eyes were enucleated, the posterior cups dissected and fixed for a total of four hours in 4% paraformaldehyde. The immunohistochemical labeling of BRN3A-positive cells was performed as previously described.[40] Briefly, the posterior cups were incubated in a 0.3% Triton-X100 solution in phosphate buffered saline (PBST) overnight at 37°C, and retinas were dissected and bleached in a 3% hydrogen peroxide solution in 1% sodium phosphate buffer for three hours at room temperature. Retinas were permeabilized for 15 minutes at –80°C in PBST, blocked in a 2% normal donkey serum in PBST overnight, immunohistochemically labeled using an anti-BRN3A antibody (1:200; sc-8429; Santa Cruz Biotechnology) in 2% normal donkey serum, 1% Triton-X 100, and 1% DMSO at 4°C for two nights, followed by incubation with a secondary antibody (1:200, Alexa Fluor 488 donkey anti-goat, Invitrogen) for four hours at room temperature, counterstained with TO-PRO-3 Iodide (1:1000, Molecular Probes), transferred to glass microscopy slides, and flat-mounted using ProLong Diamond Antifade Mountant (Fisher Scientific) and cover-slipped. Flat-mounted retinas were imaged by confocal microscopy (Zeiss LSM 710) at a total magnification of 400×. For each retina, four confocal images were collected (1024 × 1024 px, 0.18 mm^2 image area) from nonoverlapping fields in the central retina, with z-stacks of three to five images collected for each image. Images were collected from the central retina adjacent to the optic nerve head (for diagram defining the central retina, see Fig. 1 in Hedberg-Buenz et. al.[40]). Images of BRN3A-labeled nuclei were processed in ImageJ, by first z-projecting at maximum intensity, followed by the **Subtract Background** tool with rolling ball radius set to 35 pixels, followed by the **Smooth** tool. Images were then converted to binary using Huang thresholding. Binary images were further processed using the **Open**, **Watershed**, and **Fill Holes** functions. To count BRN3A-positive cells, the **Analyze Particles** function was applied to the BRN3A images with particle size set to 20 to 150 μm^2 and circularity 0 to1. Only retinas that were isolated without dissection-induced damage, such as large tears, and were fully intact were used for the purpose of this study.

Statistical Analysis

Results are expressed as mean ± standard deviation. Analysis was conducted by experimenters blinded to the treatment condition of the sample or subject. The normality of groups was validated using the D'Agostino-Pearson omnibus K2 test for normality. Groups were tested using the paired *t*-test or Student's *t*-test for samples that had the same variance, and the Welch's *t*-test (unpaired *t*-test with Welch correction) to compare samples that did not have the same variance. The variance of two groups was compared using the *F*-test of equality of variances. The significance level for *P* values was adjusted for multiple comparisons using the Bonferroni correction, which was calculated as (α/number of tests), where $\alpha = 0.05$. Correlation of baseline retinal phenotypes was performed using Pearson's Correlation Coefficient (*r*). Statistical comparisons were performed using Graphpad Prism (Ver. 8.2, Graphpad Software).

Results

Baseline Retinal Phenotypes in JDO Mice

The baseline RGC complex + RNFL thickness in J:DO mice was 70.92 ± 4.52 µm (OS, $n = 57$, Mean ± SD, coefficient of variation (CV) = 6.4%) and 71.03 ± 5.05 µm (OD, $n = 57$, CV = 7.1% Fig. 1A, Supplementary Fig. S2). The range of the RGC complex + RNFL thickness was 58.44 to 86.11 µm (OS) and 59.89 to 93.67 µm (OD). There was not a significant difference in the RGC complex + RNFL thickness between the left and right eye ($P = 0.75$, paired *t*-test). There was significant correlation between the RGC complex + RNFL

Investigative Ophthalmology & Visual Science

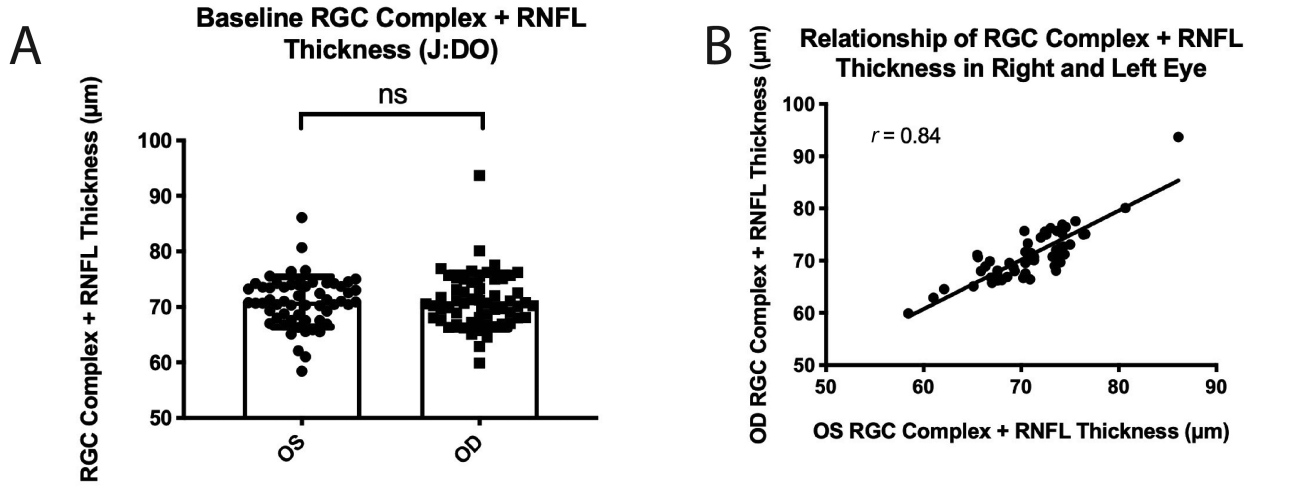

Figure 1. The thickness of the RGC complex + RNFL does not vary between the eyes of the same animal in J:DO mice. The baseline RGC complex + RNFL thickness in J:DO mice was 70.92 ± 4.52 µm (A, OS, $n = 57$, mean ± SD) and 71.03 ± 5.05 µm (OD, $n = 57$). There was not a significant difference in the RGC complex + RNFL thickness between the left and right eye ($P = 0.753$, paired t-test). There was a significant correlation between the RGC complex + RNFL thickness in the right and left eyes (B, $r = 0.84$, $P < 0.0001$).

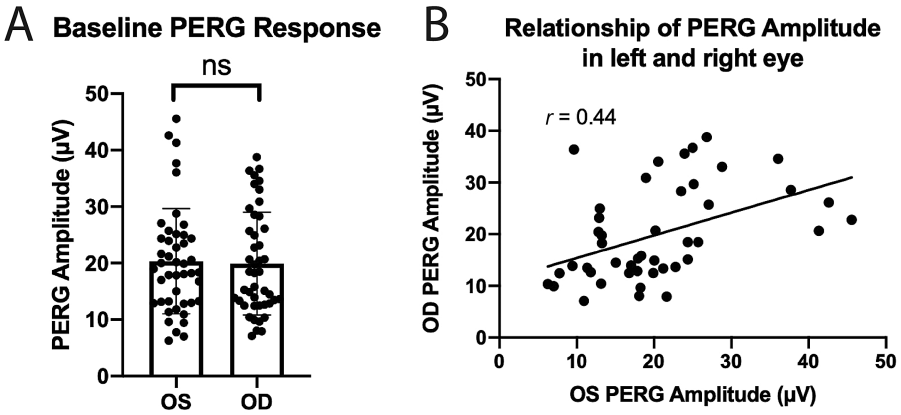

Figure 2. The RGC function assessed by PERG does not vary between each eye of the same animal in J:DO mice. The baseline PERG response in J:DO mice was 20.33 ± 9.32 µV (A, OS, $n = 45$) and 19.91 ± 9.09 µV (OD, $n = 45$). There was not a significant difference between the right and left eye ($P = 0.773$, paired t-test). There was a significant correlation between the PERG response in the right and left eye (Fig. 2 B, $r = 0.449$, $P = 0.0020$).

thickness in the right and left eyes (Fig. 1B, $r = 0.84$, $P < 0.0001$).

The RGC function was analyzed using the PERG. The average baseline PERG response in J:DO mice was 20.33 ± 9.32 µV (OS, $n = 45$, CV = 45.8%) and 19.91 ± 9.09 µV (Fig. 2A, Supplementary Fig. S3, OD, $n = 45$, CV = 45.7%). There was not a significant difference between the right and left eye ($P = 0.773$, paired t-test). There was a significant correlation between the PERG response in the right and left eye (Fig. 2B, r = 0.449, $P = 0.002$). The baseline number of RGCs in the right eye of J:DO mice was 2800 ± 241.6 RGCs/mm^2 (CV = 8.6%), with a range of 2330 to 3259 RGCs/mm^2 (Fig. 3).

We evaluated the relationship of each baseline parameter from the right eye to one another. There was a significant relationship between the baseline number of RGCs and the baseline RGC complex + RNFL thickness ($r = 0.481$, $P = 0.023$). We did not identify a relationship between the baseline RGC complex + RNFL thickness and the baseline PERG response ($r = 0.012$, $P = 0.936$). We also did not identify a relationship between the baseline PERG response and the baseline number of RGCs ($r = 0.247$, $P = 0.322$).

Phenotypic Response to Blast Exposure in J:DO Mice

For each parameter, the change in response from baseline values in each J:DO mouse was calculated four weeks following blast exposure. We observed an average change of −1.43 ± 2.88 µm (CV = 201.3%) in the RGC complex + RNFL four weeks following blast exposure, with a range of −9.77 to +14.11 µm (Fig. 4A, Supplementary Fig. S2). The baseline RGC complex + RNFL thickness in the left eye (70.92 ± 4.52 µm) was not significantly different than the postblast RGC complex + RNFL thickness (70.58 ± 7.26 µm, $P = 0.69$, paired t-test, CV = 10.2%). The average change in the PERG response of −4.14 ± 12.46 µV (CV = 300.9) with a range

Investigative Ophthalmology & Visual Science

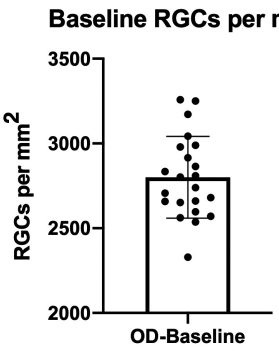

Figure 3. The baseline density of RGCs in the right eye of J:DO mice was 2800 ± 241.6 RGCs/mm^2 (n = 22), with a range of 2330 to 3259 BRN3A+ RGCs/mm^2.

of −37.57 to +15.79 µV four weeks following blast exposure (Fig. 4B, Supplementary Fig. S3). The average PERG response in J:DO mice following blast exposure (16.16 ± 7.69, CV = 47.58%) was not significantly different than the average baseline PERG response ($P = 0.07$, paired *t*-test).

Additionally, there was a change in the density of BRN3A positive cells following blast exposure. There was an average loss of 558.6 ± 440.5 BRN3A positive cells/mm^2 (CV = 78.8), with a range of −1368 to +370 four weeks following blast exposure (Fig. 4C, Supplementary Fig. S4). To validate the reliability of BRN3A labeling to detect RGCs, both the left and right eyes from C57BL/6J mice were labeled. We did not detect a difference between densities of the left (3223 ± 329.1 BRN3A-positive cells/mm^2, CV = 10.2%) and right (3298 ± 227.2 BRN3A positive cells/mm^2, CV = 6.8) eyes ($P = 0.53$, Paired *t*-test).

Phenotypic Response to Blast Exposure in Inbred Mice

In vivo retinal outcomes were analyzed in inbred mice four weeks postblast. C57BL/6J mice exposed to blast injury had an average RGC complex + RNFL thickness of 66.92 ± 1.76 µm at baseline (Fig. 5A, CV = 2.63%). The RGC complex + RNFL was 63.77 ± 1.15 µm (CV = 1.80%) and had an average change of −3.14 ± 1.09 µm (Fig. 5B, CV = 34.7%) four weeks postblast (range: −4.53 to −1.75 µm). There was a significant difference in the thickness at four weeks postblast compared to baseline values ($P = 0.0003$, paired *t*-test). Five mice from the C57BL/6J cohort were lost to follow-up due to technical difficulties with the instrument.

The baseline RGC complex + RNFL thickness for BALB/cByJ mice was 57.31 ± 2.19 µm (Fig. 5C, CV = 3.8%). The RGC complex + RNFL thickness four weeks following blast exposure was 58.15 ± 1.99 µm (CV = 3.4%). The average change in thickness from baseline was 1.02 ± 2.41 µm (CV = 236.2%) four weeks following blast exposure (Fig. 5D, range: −1.83 to +6.17 µm). There was not a significant difference between RGC complex + RNFL thickness between baseline and four weeks postblast ($P = 0.1697$, paired *t*-test). Comparison of the ΔOCT in C57BL/6J and BALB/cByJ mice showed a significantly greater decrease in C57Bl/6J mice ($P = 0.0005$, Student's *t*-test, Supplementary Fig. S5A), but not a significant difference in the variances of the groups ($F = 4.91$, $df = 11$, $P = 0.06$).

Analysis of the change in the PERG response in C57BL/6J mice showed a change of −0.25 ± 3.87 µV (CV = 1548.0%)

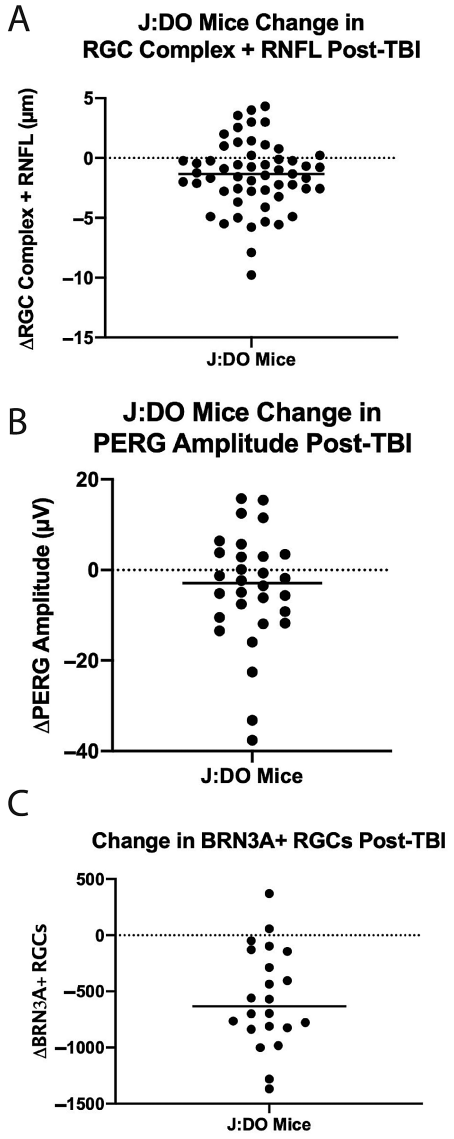

Figure 4. Phenotypic responses of J:DO mice to blast exposure. There was a change of −1.43 ± 2.88 µm in the RGC complex + RNFL thickness four weeks following blast exposure compared to baseline values, with a range of −9.77 to +14.11 µm ($n = 55$, A). There was an average change in the PERG response of −4.14 ± 12.46 µV with a range of −37.57 to +15.79 µV four weeks following blast exposure ($n = 30$, B). There was an average loss of 558.6 ± 440.5 BRN3A-positive cells/mm^2, with a range of −1368 to +370 four weeks following blast exposure (C, $n = 22$).

four weeks postblast exposure (range −6.30 to +6.30 µV), which was not significantly different between baseline (23.85 ± 3.35 µV, CV = 14.0) and four weeks postblast exposure (Fig. 5E, F, 23.60 ± 4.19 µV, CV = 17.7%, $P = 0.83$, paired *t*-test).

Blast Exposure in Outbred Mice Results in Greater Variance Compared to Inbred Mice

To understand if blast exposure resulted in differential effects in J:DO mice compared to C57BL/6J and BALB/cByJ mice, we compared the change in OCT thickness from baseline to four weeks following blast. There was a significant

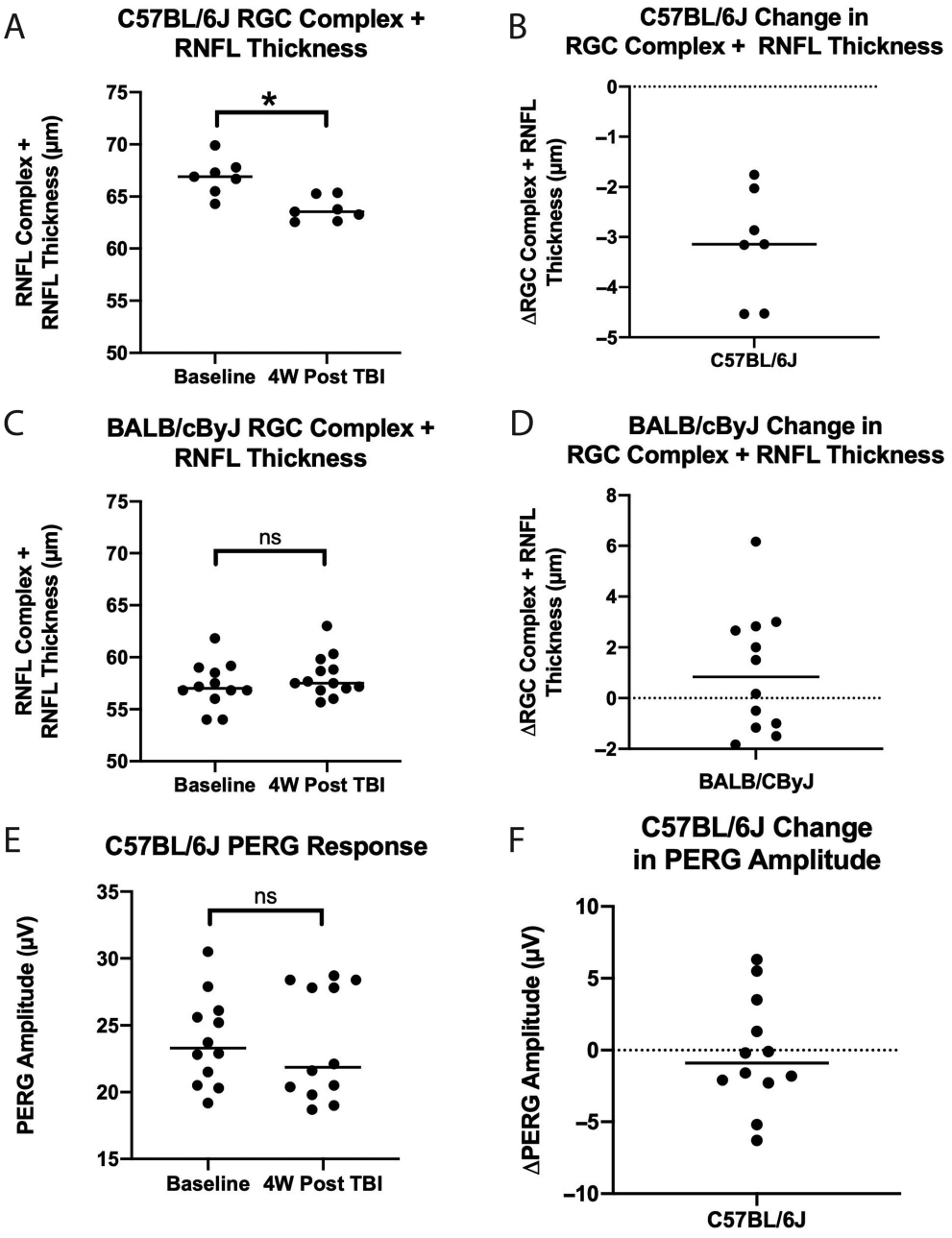

Figure 5. Phenotypic RGC responses in inbred mice. C57BL/6J mice exposed to blast injury had an average RGC complex + RNFL thickness of 66.92 ± 1.76 µm at baseline (A, $n = 7$). The RGC complex + RNFL was 63.77 + 1.15 µm and had an average change of 3.14 ± 1.09 µm four weeks postblast (B, range: −4.53 to −1.75 µm). There was a significant difference between the thickness at baseline and four weeks postblast ($P = 0.0003$, paired *t*-test). The baseline RGC complex + RNFL thickness for BALB/cByJ mice was 57.31 ± 2.19 µm (C, $n = 12$). The RGC complex thickness four weeks following blast exposure was 58.15 ± 1.99 µm. The average change in thickness from baseline was 1.02 ± 2.41 µm four weeks following blast exposure (D, range: −1.83 to +6.17 µm). There was not a significant difference between RGC complex + RNFL thickness at baseline and four weeks postblast ($P = 0.1697$, paired *t*-test). Analysis of the change in the PERG response in C57BL/6J mice showed a change of −0.25 ± 3.87 µV four weeks postblast exposure (range −6.30 to +6.30 µV), which was not significantly different between baseline (23.85 ± 3.35 µV) and four weeks postblast exposure (E, F, $n = 12$, 23.60 ± 4.19 µV, $P = 0.83$, paired *t*-test).

difference in the ΔOCT between J:DO and C57BL/6J mice ($P = 0.004$, Welch's *t*-test, Supplementary Fig. S5A), with a significant difference in the variance of the groups ($P = 0.0002$, $F = 34.86$, $df = 56$).

There was not a significant difference in the ΔPERG between J:DO and C57BL6/J ($P = 0.13$, Welch's *t*-test, Supplementary Fig. S5B), although the variances of the groups was significantly different ($P = 0.0003$, $F = 10.33$, $df = 29$). There was not a significant difference in the ΔOCT between J:DO and BALB/cByJ ($P = 0.219$, Welch's *t*-test, Supplementary Fig. S5A), although there was a significant difference in the variance of the groups ($P = 0.001$, $F = 7.10$, $df = 56$).

The raw baseline values of J:DO mice were compared to each inbred strain to understand if J:DO mice had different baseline values and a greater variance in baseline values

prior to injury. There was a significant difference in the baseline RGC complex + RNFL thickness between J:DO and C57BL/6J mice ($P = 0.0003$, Welch's *t*-test). There was also a significant difference in the variances of J:DO and C57BL/6J mice ($P = 0.03$, $F = 3.24$, df = 47). Comparison of BALB/cByJ mice and J:DO mice revealed a significant difference in baseline RGC complex + RNFL thicknesses ($P < 0.0001$), and significantly different variances ($P = 0.003$, $F = 2.77$, $df = 47$). There was also a significant difference in the RGC complex + RNFL thickness of BALB/cByJ mice compared to C57BL/6J mice ($P < 0.0001$, unpaired *t*-test), although the variances did not differ ($F = 1.53$, $df = 11$, $P = 0.62$).

Comparison of baseline PERG responses in J:DO and C57BL/6J mice showed a significant difference ($P = 0.02$, Welch's *t*-test), with significantly different variances ($P < 0.0001$, $F = 5.83$, $df = 94$). Comparison of the baseline densities of BRN3A-positive RGCs showed significantly more labeled RGCs in C57BL/6J mice compared to J:DO mice ($P < 0.0001$, Welch's *t*-test), although they did not have significantly different variances ($F = 1.13$, $df = 21$, $P = 0.85$).

Discussion

This study has demonstrated that the phenotypic RGC response to blast injury is dependent on the genetic background of the animal receiving the blast injury. We have tested the functional response of RGCs using the PERG. This analysis showed a highly variable response in outbred mice, in which the PERG amplitude increased in some J:DO mice following blast, was relatively unaffected in some mice, and was significantly decreased in others. When we compared the change in PERG amplitude from baseline in J:DO mice to C57BL/6J mice we did not observe a significant difference in the average response across all mice overall, although we did observe a significant difference in the variance of the groups. The lack of change was due to the fact that the PERG increased or did not change in some mice and decreased in many mice. Comparison of the change in the OCT thickness showed a significant difference in the amount of change between J:DO and C57BL/6J, and a significant difference in the variance of the change. In contrast, there was not a significant difference in the OCT thickness change from baseline in J:DO mice compared to BALB/cByJ, although there was a significant difference in the variances of the groups.

The results obtained in this study are in agreement with other groups that have shown an effect of neurotrauma on the visual system.[41–43] Previous studies have also shown differences among inbred strains subjected to the same blast trauma.[14,44] The differences among inbred strains are not unexpected, as previous studies of optic nerve crush have shown that RGC survival following injury is strain dependent,[45] as are RGC responses to glaucoma.[46–48] However, there appears to be differences in strain susceptibility when comparing mechanisms of injury. BALB/cByJ mice were previously shown to have the greatest susceptibility to optic nerve crush, while C57BL/6J were among the most resistant strains. In this study we have shown BALB/cByJ to be resistant to decreases in the RGC Complex + RNFL thickness. In this study (and in previous studies), we have shown the RGCs of C57BL/6J to be susceptible to blast injury.[25,26,28,29,31] The lack of a difference in OCT in the BALB/cByJ mice following blast might be due to retinal swelling or dendritic rearrangement, although these were not evaluated in this study. The differences in inbred strain responses to blast are reflected in the highly variable response in J:DO mice. While the number of mice in this study is too small to identify loci, the results presented here suggest the response to blast injury has a strong genetic component, rather than being simply the result of a physical trauma that leads to identical outcomes in all affected individuals.

Our study also has caveats that are important to note. First, we subjected mice to one single blast injury, at one blast intensity. We, and others, have previously noted that the number of blast exposures, the timing of those exposures, and the intensity of those exposures can lead to differential responses within single inbred lines of mice. An important subject of future study will be to evaluate the effect of different blast intensities on the J:DO line of mice. Second, we have only evaluated a single timepoint after blast injury in this study. Previous studies in C57BL/6J mice have shown differences in retinal responses at different timepoints after injury.[25] Future longitudinal studies in J:DO mice will be crucial to determine if the molecular mechanisms responsible for acute RGC death and dysfunction are similar or different at chronic timepoints following injury. Third, this study relied upon two noninvasive outcomes to analyze the function and structure of RGCs—the PERG and OCT. Our previous study has shown that the PERG can remain normal, while in vitro electrophysiological recordings of RGC activity show significant abnormalities that are only apparent in an intact animal when using provocative PERG for testing.[25] Future studies using provocative PERG testing, visual evoked potentials and electrophysiological single cell evaluation of RGCs will be important to understanding the relationship between RGC structure and function following blast exposure. It will also be important in future studies to analyze the functional PERG data from BALB/cByJ mice, in addition to other lines of inbred mice. Furthermore, using both pigmented mice and nonpigmented mice, as we have done in this study, will be important. This is because tyrosinase is nonfunctional in nonpigmented mice such as BALB/cByJ and is known to influence a subset of RGCs.[49] It is conceivable that this might influence the phenotypic response to TBI, which in turn may affect the variability and interpretation of the data.

Additionally, the histological analysis performed in our study relied on enucleation of one eye prior to blast exposure to provide a baseline number of RGCs. This was necessary because each J:DO mouse has a unique genetic background. It has been shown that baseline numbers of RGCs are background dependent,[39] making it likely that each J:DO mouse has a different number of baseline RGCs, which is what we detected in our study. Additionally, there is not a robust histological marker of neurodegeneration following blast injury. While there is a possibility this analysis could introduce variation, previous publications have shown that retinal parameters have high intraocular correlation in J:DO mice.[19] Furthermore, we have shown that BRN3A antibody staining is not significantly different between eyes in C57BL/6J mice. However, we cannot discount the possibility that enucleation of one eye may result in optic nerve and/or RGC damage in the fellow eye,[50] which would have the potential to influence the results presented here. Further assessment of this should be performed in future studies. Finally, our study was able to identify a contribution from genetic background, which was undoubtedly related to our ability to hold other parameters, such as the injury insult, age, and sex, constant. This finding has relevance to studies of the basic science of TBI pathophysiology, but it would be an oversimplification to assume that outcomes following

Investigative Ophthalmology & Visual Science

TBI in humans should have a pronounced link to ethnicity or heredity. The comparison of inbred mice to J:DO mice used fewer mice in the inbred groups than in the J:DO group. It will be important in subsequent studies to examine larger cohorts of mice.

In conclusion, our study has shown that there is a strong genetic component to the RGC response to blast-mediated traumatic brain injury. We have also shown significant variances in the PERG and OCT outcomes in mice of different genetic backgrounds, which indicate their utility in mapping loci and molecular pathways that contribute to the susceptibility to or preservation of RGCs following blast exposure. Identifying these genes, proteins, mechanisms, and pathways will help to develop treatments for traumatic brain injury that extend beyond blast-mediated neurotrauma, including other optic neuropathies.

Acknowledgments

Supported by the Department of Veterans Affairs Center for the Prevention and Treatment of Visual Loss, the Department of Defense (W81XWH-14-1-0583), and the U.S. Department of Veterans Affairs Rehabilitation Research and Development Service awards 1 I01 RX003389 (MMH), 1 I21 RX003325 (MMH), and IK2-RX002003 (LMD). The contents of this manuscript do not represent the views of the U.S. Department of Veterans Affairs, Department of Defense, or the U.S. Government.

Disclosure: **M.M. Harper,** None; **N. Boehme,** None; **L.M. Dutca,** None; **M.G. Anderson,** None

References

1. Taylor CA, Bell JM, Breiding MJ, Xu L. Traumatic brain injury-related emergency department visits, hospitalizations, and deaths - United States, 2007 and 2013. *MMWR Surveill Summ*. 2017;66(9):1–16.
2. Popescu C, Anghelescu A, Daia C, Onose G. Actual data on epidemiological evolution and prevention endeavours regarding traumatic brain injury. *J Med Life*. 2015;8(3):272–277.
3. Owens BD, Kragh JF, Jr., Wenke JC, Macaitis J, Wade CE, Holcomb JB. Combat wounds in operation Iraqi Freedom and operation Enduring Freedom. *J Trauma*. 2008;64(2):295–299.
4. Murray CK, Reynolds JC, Schroeder JM, Harrison MB, Evans OM, Hospenthal DR. Spectrum of care provided at an echelon II Medical Unit during Operation Iraqi Freedom. *Mil Med*. 2005;170(6):516–520.
5. Cho RI, Bakken HE, Reynolds ME, Schlifka BA, Powers DB. Concomitant cranial and ocular combat injuries during Operation Iraqi Freedom. *J Trauma*. 2009;67(3):519–520; discussion 9–20.
6. Cockerham GC, Goodrich GL, Weichel ED, Orcutt JC, Rizzo JF, Bower KS, Schuchard RA. Eye and visual function in traumatic brain injury. *J Rehabil Res Dev*. 2009;46(6):811–818.
7. Reynolds ME, Barker FM, 2nd, Merezhinskaya N, Oh GT, Stahlman S. Incidence and temporal presentation of visual dysfunction following diagnosis of traumatic brain injury, active component, U.S. Armed Forces, 2006-2017. *MSMR*. 2019;26(9):13–24.
8. Schwab KA, Gudmudsson LS, Lew HL. Long-term functional outcomes of traumatic brain injury. *Handb Clin Neurol*. 2015;128:649–659.
9. Weaver SM, Portelli JN, Chau A, Cristofori I, Moretti L, Grafman J. Genetic polymorphisms and traumatic brain injury: the contribution of individual differences to recovery. *Brain Imaging Behav*. 2014;8(3):420–434.
10. Weaver SM, Portelli JN. Neurobiological influences on recovery from traumatic brain injury: the role of genetic polymorphisms. *Curr Pharm Des*. 2014;20(26):4275–4283.
11. McAllister TW. Genetic factors in traumatic brain injury. *Handb Clin Neurol*. Waltham, MA, Elsiver B.V, 2015;128:723–739.
12. Weaver SM, Chau A, Portelli JN, Grafman J. Genetic polymorphisms influence recovery from traumatic brain injury. *Neuroscientist*. 2012;18(6):631–9644.
13. McDevitt J, Krynetskiy E. Genetic findings in sport-related concussions: potential for individualized medicine? *Concussion*. 2017;2(1):CNC26.
14. Bricker-Anthony C, Rex TS. Neurodegeneration and vision loss after mild blunt trauma in the C57Bl/6 and DBA/2J mouse. *PLoS One*. 2015;10(7):e0131921.
15. Struebing FL, King R, Li Y, Chrenek MA, Lyuboslavsky PN, Sidhu CS, Iuvone PM, Geisert EE. Transcriptional changes in the mouse retina after ocular blast injury: a role for the immune system. *J Neurotrauma*. 2018;35(1):118–129.
16. Threadgill DW, Miller DR, Churchill GA, de Villena FP. The collaborative cross: a recombinant inbred mouse population for the systems genetic era. *ILAR J*. 2011;52(1):24–31.
17. Mattapallil MJ, Wawrousek EF, Chan CC, et al.The Rd8 mutation of the Crb1 gene is present in vendor lines of C57BL/6N mice and embryonic stem cells, and confounds ocular induced mutant phenotypes. *Invest Ophthalmol Vis Sci*. 2012;53(6):2921–2927.
18. Chang B, Hawes NL, Hurd RE, Davisson MT, Nusinowitz S, Heckenlively JR. Retinal degeneration mutants in the mouse. *Vision Res*. 2002;42(4):517–525.
19. Hedberg-Buenz A, Meyer KJ, van der Heide CJ, et al. Biological correlations and confounding variables for quantification of retinal ganglion cells based on optical coherence tomography using diversity outbred mice. bioRxiv. 2020.12.23.423848.
20. Svenson KL, Gatti DM, Valdar W, et al. High-resolution genetic mapping using the Mouse Diversity outbred population. *Genetics*. 2012;190(2):437–447.
21. Philip VM, Sokoloff G, Ackert-Bicknell CL, et al. Genetic analysis in the Collaborative Cross breeding population. *Genome Res*. 2011;21(8):1223–1238.
22. Solberg Woods LC. QTL mapping in outbred populations: successes and challenges. *Physiol Genomics*. 2014;46(3):81–90.
23. Churchill GA, Gatti DM, Munger SC, Svenson KL. The Diversity Outbred mouse population. *Mamm Genome*. 2012;23(9-10):713–718.
24. Gatti DM, Svenson KL, Shabalin A, et al. Quantitative trait locus mapping methods for diversity outbred mice. *G3 (Bethesda)*. 2014;4(9):1623–1633.
25. Dutca LM, Stasheff SF, Hedberg-Buenz A, et al. Early detection of subclinical visual damage after blast-mediated TBI enables prevention of chronic visual deficit by treatment with P7C3-S243. *Invest Ophthalmol Vis Sci*. 2014;55(12):8330–8341.
26. Mohan K, Kecova H, Hernandez-Merino E, Kardon RH, Harper MM. Retinal ganglion cell damage in an experimental rodent model of blast-mediated traumatic brain injury. *Invest Ophthalmol Vis Sci*. 2013;54(5):3440–3450.
27. Harper MM, Rudd D, Meyer KJ, et al. Identification of chronic brain protein changes and protein targets of serum auto-antibodies after blast-mediated traumatic brain injury. *Heliyon*. 2020;6(2):e03374.
28. Evans LP, Woll AW, Wu S, et al. Modulation of post-traumatic immune response using the IL-1 receptor antagonist

anakinra for improved visual outcomes. *J Neurotrauma*. 2020;37(12):1463–1480, doi:10.1089/neu.2019.6725.

29. Evans LP, Boehme N, Wu S, et al. Sex does not influence visual outcomes after blast-mediated traumatic brain injury but IL-1 pathway mutations confer partial rescue. *Invest Ophthalmol Vis Sci*. 2020;61(12):7.
30. Harper MM, Hedberg-Buenz A, Herlein J, et al. Blast-mediated traumatic brain injury exacerbates retinal damage and amyloidosis in the APPswePSENd19e mouse model of Alzheimer's Disease. *Invest Ophthalmol Vis Sci*. 2019;60(7):2716–2725.
31. Harper MM, Woll AW, Evans LP, et al. Blast preconditioning protects retinal ganglion cells and reveals targets for prevention of neurodegeneration following blast-mediated traumatic brian injury. *Invest Ophthalmol Vis Sci*. 2019;60(13):4159–4170.
32. Yin TC, Voorhees JR, Genova RM, Davis KC, Madison AM, Britt JK, Cintrón-Pérez CJ, McDaniel L, Harper MM, Pieper AA. Acute axonal degeneration drives development of cognitive, motor, and visual deficits after blast-mediated traumatic brain injury in mice. *eNeuro*. 2016;3(5):ENEURO.0220-16.2016, doi:10.1523/ENEURO.0220-16.2016.
33. Yin TC, Britt JK, De Jesus-Cortes H, et al. P7C3 neuroprotective chemicals block axonal degeneration and preserve function after traumatic brain injury. *Cell Rep*. 2014;8(6):1731–1740.
34. Chou TH, Bohorquez J, Toft-Nielsen J, Ozdamar O, Porciatti V. Robust mouse pattern electroretinograms derived simultaneously from each eye using a common snout electrode. *Invest Ophthalmol Vis Sci*. 2014;55(4):2469–2475.
35. Mohan K, Harper MM, Kecova H, et al. Characterization of structure and function of the mouse retina using pattern electroretinography, pupil light reflex, and optical coherence tomography. *Vet Ophthalmol*. 2012;15(Suppl 2):94–104.
36. Evans LP, Woll AW, Wu S, et al. Modulation of post-traumatic immune response using the IL-1 receptor antagonist anakinra for improved visual outcomes. *J Neurotrauma*. 2020;37(12):1463–1480.
37. Mohan K, Kecova H, Hernandez-Merino E, et al. Retinal ganglion cell damage in an experimental rodent model of blast-mediated traumatic brain injury. *Invest Ophthalmol Visual Sci*. 2013;54(5):3440–3450.
38. Saul MC, Philip VM, Reinholdt LG. Center for Systems Neurogenetics of Addiction, Chesler EJ. High-diversity mouse populations for complex traits. *Trends Genet*. 2019;35(7):501–514.
39. Williams RW, Strom RC, Rice DS, Goldowitz D. Genetic and environmental control of variation in retinal ganglion cell number in mice. *J Neurosci*. 1996;16(22):7193–7205.
40. Hedberg-Buenz A, Christopher MA, Lewis CJ, et al. RetFM-J, an ImageJ-based module for automated counting and quantifying features of nuclei in retinal whole-mounts. *Exp Eye Res*. 2016;146:386–392.
41. Tzekov R, Dawson C, Orlando M, et al. Sub-chronic neuropathological and biochemical changes in mouse visual system after repetitive mild traumatic brain injury. *PLoS One*. 2016;11(4):e0153608.
42. Shedd DF, Benko NA, Jones J, Zaugg BE, Peiffer RL, Coats B. Long term temporal changes in structure and function of rat visual system after blast exposure. *Invest Ophthalmol Vis Sci*. 2018;59(1):349–361.
43. Allen RS, Motz CT, Feola A, et al. Long-term functional and structural consequences of primary blast overpressure to the eye. *J Neurotrauma*. 2018;35(17):2104–2116.
44. Bricker-Anthony C, Hines-Beard J, D'Surney L, Rex TS. Exacerbation of blast-induced ocular trauma by an immune response. *J Neuroinflammation*. 2014;11:192.
45. Li Y, Semaan SJ, Schlamp CL, Nickells RW. Dominant inheritance of retinal ganglion cell resistance to optic nerve crush in mice. *BMC Neurosci*. 2007;8:19.
46. Mao M, Hedberg-Buenz A, Koehn D, John SW, Anderson MG. Anterior segment dysgenesis and early-onset glaucoma in nee mice with mutation of Sh3pxd2b. *Invest Ophthalmol Vis Sci*. 2011;52(5):2679–2688.
47. Anderson MG, Libby RT, Mao M, et al. Genetic context determines susceptibility to intraocular pressure elevation in a mouse pigmentary glaucoma. *BMC Biol*. 2006;4:20.
48. Anderson MG, Smith RS, Savinova OV, et al. Genetic modification of glaucoma associated phenotypes between AKXD-28/Ty and DBA/2J mice. *BMC Genet*. 2001;2:1.
49. Guillery RW. Visual pathways in albinos. *Sci Am*. 1974;230(5):44–54.
50. Lucas-Ruiz F, Galindo-Romero C, Rodriguez-Ramirez KT, Vidal-Sanz M, Agudo-Barriuso M. Neuronal death in the contralateral un-injured retina after unilateral axotomy: Role of microglial cells. *Int J Mol Sci*. 2019;20(22):5733, https://doi.org/10.3390/ijms20225733.

Investigative Ophthalmology & Visual Science